

## Galactic Orbits of Selected Companions of the Milky Way

A.T. Bajkova, V.V. Bobylev

*Central (Pulkovo) Astronomical Observatory, Russian Academy of Sciences, Pulkovskoe shosse 65, St. Petersburg, 196140 Russia*

**Abstract**—High-accuracy absolute proper motions, radial velocities, and distances have now been measured for a number of dwarf-galaxy companions of the Milky Way, making it possible to study their 3D dynamics. Galactic orbits for 11 such galaxies (Fornax, Sagittarius, Ursa Minor, LMC, SMC, Sculptor, Sextans, Carina, Draco, Leo I, Leo II) have been derived using two previously refined models for the Galactic potential with the Navarro–Frenk–White and Allen–Santillán expressions for the potential of the dark-matter halo, and two different masses for the Galaxy within 200 kpc— $0.75 \times 10^{12} M_{\odot}$  and  $1.45 \times 10^{12} M_{\odot}$ . The character of the orbits of most of these galaxies indicates that they are tightly gravitationally bound to the Milky Way, even with the lower-mass model for the gravitational potential. One exception is the most distant galaxy in the list, Leo I, whose orbit demonstrates that it is only weakly gravitationally bound, even using the higher-mass model of the gravitational potential.

DOI: 10.1134/S1063772917080017

## 1 INTRODUCTION

With a size of about 1000 kpc, the Local Group contains more than 60 galaxies [1], with the Andromeda Galaxy and the Milky Way dominating. Each of these two galaxies is surrounded by a cloud of companion galaxies. The following estimated masses for the Local Group (LG), Andromeda Galaxy (M31), and Milky Way (MW) were derived in [2] from data on the Local Group galaxies, assuming that the group is in equilibrium:  $M_{LG} = (2.5 \pm 0.4) \times 10^{12} M_{\odot}$ ,  $M_{M31} = (1.7 \pm 0.3) \times 10^{12} M_{\odot}$  and  $M_{MW} = (0.8 \pm 0.5) \times 10^{12} M_{\odot}$ .

The volume bounded by the virial radius of the Milky Way,  $r_{vir} \sim 300$  kpc, contains more than 40 known dwarf galaxies [3]. Analysis of the distances and radial velocities of dwarf galaxies in this volume indicates that they are gravitationally bound to the Milky Way. One exception is one of the most distant galaxies of the group, Leo I [1,4,5]. Using the total space velocities of the galaxies can clarify the question of whether Local Group members are gravitationally bound, and hence of the mass of the Milky Way. However, unlike uncertainties in radial velocities, proper motion uncertainties depend on the distance, so that angular measurements with very high accuracy are needed.

Nevertheless, analysis of the total space velocities of several dwarf galaxies that are companions to the Milky Way have been repeatedly performed by different sets of authors with different aims [6–8]. For example, it was found that the estimate of the total mass of the Milky Way depends considerably on the dwarf galaxy Leo I [4]; the question of whether

the dwarf galaxy Leo II is gravitationally bound to the Milky Way was considered in [9]; the frequency of mutual collisions of the companion galaxies was estimated in [6]; and the most probable mass of the Galaxy within a sphere 200 kpc in radius was estimated to be  $M_{200} = 1.1 \times 10^{12} M_{\odot}$  [8].

The absolute proper motions of several dwarf companions of the Milky Way were measured using the Hubble Space Telescope (HST). These data, together with ground-based observations, are collected in [10]. Analyzing these data is of considerable interest for studying the dynamics of the Local Group of galaxies [11].

In [12], we re-determined parameters of the three most popular three-component (bulge, halo, disk) axially symmetric models for the Galaxy's gravitational potential, which differ in the type of expression used for the dark-matter halo, namely, the expressions of Allen and Santillán (I) [13], Wilkinson and Evans (II) [14], and Navarro, Frenk, and White (III) [15]. In all these models, the bulge and disk are described using expressions from Miyamoto and Nagai [16]. We used various modern observations over a wide range of Galactocentric distances  $R$  between 0 and 200 kpc. For distances of about 20 kpc, we used radial velocities of hydrogen clouds at tangential points and data on 130 masers with measured trigonometric parallaxes; at larger distances, we used averaged rotation velocities for a variety of objects (carbon stars, giants, globular clusters, and dwarf galaxies) from the survey [17]. We fitted the observed velocities with model rotation curves taking into account limits for the local density of matter and the vertical force. It is important to note that the models we obtained correspond to different total masses for the Galaxy. The Galaxy's mass within 200 kpc is highest for Model I,  $M_G(R \leq 200 \text{ kpc}) = (1.45 \pm 0.30) \times 10^{12} M_{\odot}$ , and lowest for Model II,  $M_G(R \leq 200 \text{ kpc}) = (0.61 \pm 0.12) \times 10^{12} M_{\odot}$ . Model III can be considered the best of the models considered, as it provides the lowest residuals between the data and the model rotation curve. The Galaxy's mass in Model III  $M_G(R \leq 200 \text{ kpc}) = (0.75 \pm 0.19) \times 10^{12} M_{\odot}$ .

Since the positions and velocities of the listed dwarf companion galaxies are continuously being refined, it is of considerable interest to analyze their 3D dynamics using the refined Galactic potential in order to establish the extent to which the companion galaxies are bound to our Galaxy. This is the subject of the present study.

## 2 DATA

The most important source of data for our study is [10], in which mean proper motions are derived for 11 galactic companions of the Milky Way. For each of these galaxies, from one to four independent measurements of absolute proper motions were used, at least one derived from HST observations. The galaxies' coordinates, distances, and radial velocities from [1] were used in [10].

Our list contains 11 dwarf-galaxy companions of the Milky Way: Fornax, Sagittarius, Ursa Minor, LMC, SMC, Sculptor, Sextans, Carina, Draco, Leo I, Leo II. The data for seven of these galaxies were taken directly from [10] and [1].

We derived new mean absolute proper motions for Draco, using two independent determinations of the absolute proper motions for this galaxy. The first resulted from the reduction of HST observations:  $\mu_{\alpha} \cos \delta = 0.177 \pm 0.063$  milliarcsec/year (mas/year) and  $\mu_{\delta} = -0.221 \pm 0.063$  mas/year [18]. The second measurement is based on ground-based observations with the Subaru telescope:  $\mu_{\alpha} \cos \delta = -0.284 \pm 0.047$  mas/year and  $\mu_{\delta} = -0.289 \pm 0.014$  mas/year [19]. The mean of these two measurements is  $\mu_{\alpha} \cos \delta = -0.054 \pm 0.055$  mas/year

Table 1: Data used for companion galaxies of the Milky Way

Galaxy	$l$ , deg	$b$ , deg	$\mu_\alpha \cos \delta$ , mas/year	$\mu_\delta$ , mas/year	$V_r$ , km/s	$d$ , kpc
Sgr	5.57	-14.17	$-2.684 \pm 0.200$	$-1.015 \pm 0.070$	$140.0 \pm 2.0$	$26 \pm 2$
LMC	280.47	-32.89	$1.903 \pm 0.014$	$0.235 \pm 0.026$	$262.2 \pm 3.4$	$50 \pm 3$
SMC	302.81	-44.33	$0.723 \pm 0.025$	$-1.172 \pm 0.044$	$145.6 \pm 0.6$	$64 \pm 4$
Draco	86.37	+34.71	$-0.054 \pm 0.055$	$-0.255 \pm 0.042$	$-293.3 \pm 1.0$	$82 \pm 6$
UMi	104.95	+44.80	$-0.036 \pm 0.071$	$0.144 \pm 0.083$	$-246.9 \pm 0.1$	$76 \pm 3$
Sculptor	287.53	-83.16	$0.168 \pm 0.104$	$-0.036 \pm 0.112$	$111.4 \pm 0.1$	$86 \pm 6$
Sextans	243.50	+42.27	$-0.260 \pm 0.410$	$0.100 \pm 0.440$	$224.2 \pm 0.1$	$86 \pm 4$
Carina	260.11	-22.22	$0.220 \pm 0.090$	$0.150 \pm 0.090$	$222.9 \pm 0.1$	$105 \pm 6$
Fornax	237.25	-65.66	$0.493 \pm 0.041$	$-0.351 \pm 0.037$	$53.3 \pm 0.8$	$139 \pm 8$
Leo II (a)	220.17	+67.23	$0.104 \pm 0.113$	$-0.033 \pm 0.151$	$78.0 \pm 0.1$	$233 \pm 14$
Leo II (b)	220.17	+67.23	$-0.069 \pm 0.037$	$-0.087 \pm 0.039$	$79.0 \pm 0.6$	$233 \pm 15$
Leo I	225.99	+49.11	$-0.114 \pm 0.030$	$-0.126 \pm 0.029$	$282.9 \pm 0.5$	$257 \pm 13$

and  $\mu_\delta = -0.255 \pm 0.042$  mas/year. We adopted the heliocentric distance  $d = 82.4 \pm 5.8$  kpc from the estimate [20], based on an analysis of 270 RR Lyrae variables, and the heliocentric radial velocity  $V_r = -293.3 \pm 1.0$  km/s [21].

We used the new mean proper motions for the Magellanic Clouds (LMC and SMC) from [22]. These are based on observations with the HST [23] and an analysis of stellar proper motions from the Gaia DR1 catalog [24, 25].

Two sets of measurements are available for the dwarf galaxy Leo II, which we decided not to average. The absolute proper motions of this galaxy were obtained in [9] using HST data with an epoch difference of about 14 years:  $\mu_\alpha \cos \delta = 0.104 \pm 0.113$  mas/year and  $\mu_\delta = -0.033 \pm 0.151$  mas/year. When computing these values, measurements of 3224 stars and 17 galaxies were used to derive the absolute motions. We took the coordinates, radial velocity  $V_r = 78.0 \pm 0.1$  km/s, and distance  $d = 233 \pm 14$  kpc from [1]. We will refer to this data set as Leo II (a).

The absolute proper motions of Leo II were also measured in [26] from HST data with an epoch difference of about 2 years:  $\mu_\alpha \cos \delta = -0.069 \pm 0.037$  mas/year and  $\mu_\delta = -0.087 \pm 0.039$  mas/year. The reduction to absolute proper motions was based on measurements of more than 100 background galaxies and two quasars. Piatek et al. [26] used the radial velocity  $V_r = 79.1 \pm 0.6$  km/s [27] and distance  $d = 233 \pm 15$  kpc [28] for Leo II. They suggested that they had achieved higher accuracy in their study by averaging six independent measurements. We will refer to this data set as Leo II (b). These two data sets have considerably different proper motions and random errors, leading to our decision to consider both.

The basic parameters of the 11 dwarf galaxies are collected in Table 1, whose columns contain each galaxy’s (1) name, (2)–(3) Galactic coordinates  $l$  and  $b$ , (4)–(5) proper motions  $\mu_\alpha \cos \delta$  and  $\mu_\delta$ , (6) heliocentric radial velocity  $V_r$ , and (7) heliocentric distance  $d$ .

Table 2: Parameters of Models I and III for the Galactic potential according to [12], for  $M_{gal} = 2.325 \times 10^7 M_{\odot}$

Parameter	Model I	Model III
$M_b(M_{gal})$	$386 \pm 10$	$443 \pm 27$
$M_d(M_{gal})$	$3092 \pm 62$	$2798 \pm 84$
$M_h(M_{gal})$	$452 \pm 83$	$12474 \pm 3289$
$b_b(\text{kpc})$	$0.2487 \pm 0.0060$	$0.2672 \pm 0.0090$
$a_d(\text{kpc})$	$3.67 \pm 0.16$	$4.40 \pm 0.73$
$b_d(\text{kpc})$	$0.3049 \pm 0.0028$	$0.3084 \pm 0.0050$
$a_h(\text{kpc})$	$1.52 \pm 0.18$	$7.7 \pm 2.1$

Table 3: Initial velocities (in km/s) in the fixed Cartesian  $U, V, W$  and cylindrical  $\Pi, \Theta$  coordinates

Galaxy	$U$	$V$	$W$	$\Pi$	$\Theta$
Sgr	$232 \pm 2$	$30 \pm 25$	$219 \pm 26$	$234 \pm 4$	$3 \pm 25$
LMC	$-42 \pm 11$	$-217 \pm 11$	$229 \pm 16$	$217 \pm 11$	$38 \pm 11$
SMC	$20 \pm 23$	$-158 \pm 23$	$161 \pm 18$	$154 \pm 23$	$44 \pm 23$
Draco	$93 \pm 17$	$-6 \pm 15$	$-137 \pm 19$	$-12 \pm 15$	$92 \pm 17$
UMi	$7 \pm 4$	$94 \pm 26$	$-186 \pm 28$	$83 \pm 24$	$43 \pm 11$
Sculptor	$-34 \pm 61$	$193 \pm 46$	$-99 \pm 4$	$-155 \pm 50$	$121 \pm 58$
Sextans	$-168 \pm 100$	$118 \pm 160$	$117 \pm 180$	$-9 \pm 145$	$206 \pm 121$
Carina	$-73 \pm 27$	$13 \pm 15$	$39 \pm 52$	$6 \pm 16$	$74 \pm 26$
Fornax	$-35 \pm 11$	$-130 \pm 7$	$107 \pm 12$	$123 \pm 8$	$-55 \pm 9$
Leo II (a)	$112 \pm 197$	$254 \pm 199$	$109 \pm 51$	$-253 \pm 198$	$115 \pm 198$
Leo II (b)	$-40 \pm 56$	$124 \pm 54$	$41 \pm 21$	$-43 \pm 55$	$123 \pm 54$
Leo I	$-168 \pm 37$	$-32 \pm 38$	$94 \pm 33$	$143 \pm 38$	$93 \pm 38$

## 3 METHOD

### 3.1 Model for the Galactic Potential

The axially symmetric gravitational potential of the Galaxy was represented as the sum of three components — the central, spherical bulge  $\Phi_b(r(R, Z))$ , the disk  $\Phi_d(r(R, Z))$ , and the massive, spherical dark-matter halo  $\Phi_h(r(R, Z))$ :

$$\Phi(R, Z) = \Phi_b(r(R, Z)) + \Phi_d(r(R, Z)) + \Phi_h(r(R, Z)). \quad (1)$$

Here, we used a cylindrical coordinate system  $(R, \psi, Z)$  with its origin at the Galactic center. In Cartesian coordinates  $(X, Y, Z)$  with their origin at the Galactic center, the distance to a star (the spherical radius) is  $r^2 = X^2 + Y^2 + Z^2 = R^2 + Z^2$ , where the  $X$  axis is directed from the Sun toward the Galactic center, the  $Y$  axis is perpendicular to the  $X$  axis and points in the direction of the Galactic rotation, and the  $Z$  axis is perpendicular to the Galactic  $(XY)$  plane and points in the direction of the North Galactic pole. The gravitational potential is expressed in units of  $100 \text{ km}^2 \text{ s}^{-2}$ , distances in kpc, masses in units of the mass of the Galaxy,  $M_{gal} = 2.325 \times 10^7 M_{\odot}$ , and the gravitational constant is taken to be  $G = 1$ .

Table 4: Parameters of the orbits of the dwarf-galaxy companions of the Milky Way, shown in Figs. 1–4 for Model III (top) and Model I (bottom).

Galaxy	$a_{min}$ kpc	$a_{max}$ kpc	$e$
Sgr	15	56	0.58
LMC	50	912	0.90
SMC	61	136	0.38
Draco	46	119	0.45
UMi	68	170	0.43
Sculptor	75	268	0.57
Sextans	82	460	0.70
Carina	29	107	0.57
Fornax	129	286	0.38
Leo II (a)	234	2457	0.83
Leo II (b)	225	362	0.23
Leo I	98	1245	0.85
LMC	48	225	0.65
Leo I	79	975	0.85

We expressed the potentials of the bulge,  $\Phi_b(r(R, Z))$ , and disk,  $\Phi_d(r(R, Z))$ , in the form suggested by Miyamoto and Nagai [16]:

$$\Phi_b(r) = -\frac{M_b}{(r^2 + b_b^2)^{1/2}}, \quad (2)$$

$$\Phi_d(R, Z) = -\frac{M_d}{\left[ R^2 + \left( a_d + \sqrt{Z^2 + b_d^2} \right)^2 \right]^{1/2}}, \quad (3)$$

where  $M_b, M_d$  are the masses of these components, and  $b_b, a_d, b_d$  are the scale parameters of the components in kpc. For the halo component, we used the expression presented in [15]:

$$\Phi_h(r) = -\frac{M_h}{r} \ln \left( 1 + \frac{r}{a_h} \right). \quad (4)$$

The right column of Table 2 presents the model parameters of the Galactic potential (2)–(4) computed in [12] using the rotation velocities of Galactic objects at distances  $R$  within  $\sim 200$  kpc. Note that the corresponding Galactic rotation curve was derived using the local parameters  $R_\odot = 8.3$  kpc and  $V_\odot = 244$  km/s.

The model (2)–(4) is called Model III in [12]. In our present study, Model III is our main model, and is regarded to be optimal from the point of view of its fit to the observations. Because of this, we computed almost all the dwarf-galaxy orbits using this particular model. In the model, the total mass of the Galaxy within a sphere of radius 200 kpc is  $M_{200} = (0.75 \pm 0.19) \times 10^{12} M_\odot$ .

Model II of Wilkinson and Evans, also considered in [12], is close to Model III. The total mass of the Galaxy in this model is comparable to the mass for Model III,  $M_{200} =$

Table 5: Orbital characteristics of the dwarf-galaxy companions of the Milky Way, computed taking into account the uncertainties in the input data and the parameters of the gravitational potential for Model III (top) and Model I (bottom).

Galaxy	$a_{min}$ kpc	$a_{max}$ kpc	$e$
Sgr	$15 \pm 2$	$62 \pm 22$	$0.59 \pm 0.07$
LMC	$48 \pm 2$	$920 \pm 408$	$0.88 \pm 0.07$
SMC	$60 \pm 3$	$160 \pm 75$	$0.41 \pm 0.15$
Draco	$45 \pm 8$	$122 \pm 23$	$0.45 \pm 0.06$
UMi	$68 \pm 7$	$218 \pm 100$	$0.48 \pm 0.13$
Sculptor	$71 \pm 13$	$450 \pm 432$	$0.61 \pm 0.16$
Sextans	$73 \pm 21$	$1933 \pm 1374$	$0.83 \pm 0.08$
Carina	$38 \pm 28$	$112 \pm 13$	$0.54 \pm 0.23$
Fornax	$121 \pm 21$	$363 \pm 209$	$0.44 \pm 0.14$
Leo II (a)	$221 \pm 32$	$2521 \pm 1185$	$0.81 \pm 0.09$
Leo II (b)	$192 \pm 60$	$573 \pm 378$	$0.44 \pm 0.18$
Leo I	$103 \pm 35$	$1323 \pm 289$	$0.85 \pm 0.05$
LMC	$48 \pm 2$	$239 \pm 79$	$0.65 \pm 0.08$
Leo I	$78 \pm 30$	$997 \pm 348$	$0.84 \pm 0.07$

$(0.61 \pm 0.12) \times 10^{12} M_{\odot}$ . The similarity of Models II and III can be demonstrated by integrating the orbits of selected globular clusters.

For this reason, Model II is not very important for us, and we do not consider it farther. Model I [12] is far more interesting for us, as it features a total mass of the Galaxy within 200 kpc that is almost twice as large:  $M_{200} = (1.45 \pm 0.30) \times 10^{12} M_{\odot}$ . In this model, the potential of the dark matter halo is expressed [29] as:

$$\Phi_h(r) = \begin{cases} \frac{M_h}{a_h} \left( \frac{1}{(\gamma-1)} \ln \left( \frac{1 + (r/a_h)^{\gamma-1}}{1 + (\Lambda/a_h)^{\gamma-1}} \right) - \frac{(\Lambda/a_h)^{\gamma-1}}{1 + (\Lambda/a_h)^{\gamma-1}} \right), & \text{if } r \leq \Lambda, \\ -\frac{M_h}{r} \frac{(\Lambda/a_h)^{\gamma}}{1 + (\Lambda/a_h)^{\gamma-1}}, & \text{if } r > \Lambda, \end{cases} \quad (5)$$

where  $M_h$  is the mass and  $a_h$  a scaling parameter, the distance from the Galactic center is taken to be  $\Lambda = 200$  kpc, and the dimensionless coefficient is  $\gamma = 2.0$ . The parameters of this model are also given in Table 2. With Eqs. (2)–(3) taken into account, we have a modification of the model of Allen and Santillán [13]. We applied this model to analyze the orbits of the Large Magellanic Cloud (LMC) and the most distant dwarf galaxy in our list, Leo I.

### 3.2 Construction of the Orbits

The equation of motion of a test particle in an axially symmetric gravitational potential can be obtained from the Lagrangian of the system  $\mathcal{L}$  (see Appendix A in [29]):

$$\mathcal{L}(R, Z, \dot{R}, \dot{\psi}, \dot{Z}) = 0.5(\dot{R}^2 + (R\dot{\psi})^2 + \dot{Z}^2) - \Phi(R, Z). \quad (6)$$

Introducing the canonical moments

$$\begin{aligned} p_R &= \partial\mathcal{L}/\partial\dot{R} = \dot{R}, \\ p_\psi &= \partial\mathcal{L}/\partial\dot{\psi} = R^2\dot{\psi}, \\ p_Z &= \partial\mathcal{L}/\partial\dot{Z} = \dot{Z}, \end{aligned} \quad (7)$$

we obtain the Lagrangian equations in the form of a system of six first-order differential equations:

$$\begin{aligned} \dot{R} &= p_R, \\ \dot{\psi} &= p_\psi/R^2, \\ \dot{Z} &= p_Z, \\ \dot{p}_R &= -\partial\Phi(R, Z)/\partial R + p_\psi^2/R^3, \\ \dot{p}_\psi &= 0, \\ \dot{p}_Z &= -\partial\Phi(R, Z)/\partial Z. \end{aligned} \quad (8)$$

We integrated Eqs. (8) using a fourth-order Runge-Kutta algorithm.

The Sun's peculiar velocity with respect to the Local Standard of Rest was taken to be  $(u_\odot, v_\odot, w_\odot) = (11.1, 12.2, 7.3) \pm (0.7, 0.5, 0.4)$  km/s [30]. Here, we used the heliocentric velocities in a moving Cartesian coordinate system with  $u$  directed towards the Galactic center,  $v$  in the direction of the Galactic rotation, and  $w$  perpendicular to the Galactic plane and directed towards the north Galactic pole.

Let us denote the initial positions and proper motions of a test particle in the Galactocentric coordinate system as  $(x_o, y_o, z_o, u_o, v_o, w_o)$ . The initial positions and velocities of a test particle in the Cartesian Galactic coordinate system are then given by the formulas:

$$\begin{aligned} X &= R_0 - x_o, Y = y_o, Z = z_o, \\ U &= u_o + u_\odot, \\ V &= v_o + v_\odot + V_0, \\ W &= w_o + w_\odot, \\ \Pi &= -U \cos \psi_o + V \sin \psi_o, \\ \Theta &= U \sin \psi_o + V \cos \psi_o, \end{aligned} \quad (9)$$

where  $R_0$  and  $V_0$  are the Galactocentric distance and the linear velocity of the Local Standard of Rest around the Galactic center, and  $\tan \psi_o = Y/X$ .

The initial space velocities  $U, V, W$  and the velocities  $\Pi$  and  $\Theta$  along the  $R$  and  $\psi$  cylindrical coordinates are collected in Table 3. Table 4 presents the perigalactic,  $a_{min}$ , and apogalactic,  $a_{max}$ , distances and eccentricities  $e$  of the derived orbits of the dwarf companion galaxies.

### 3.3 RESULTS AND DISCUSSION

The Galactic orbits of all 11 dwarf galaxies are displayed in Figs. 1–4. We show two projections for each of the galaxies, onto the  $XY$  and  $RZ$  planes.

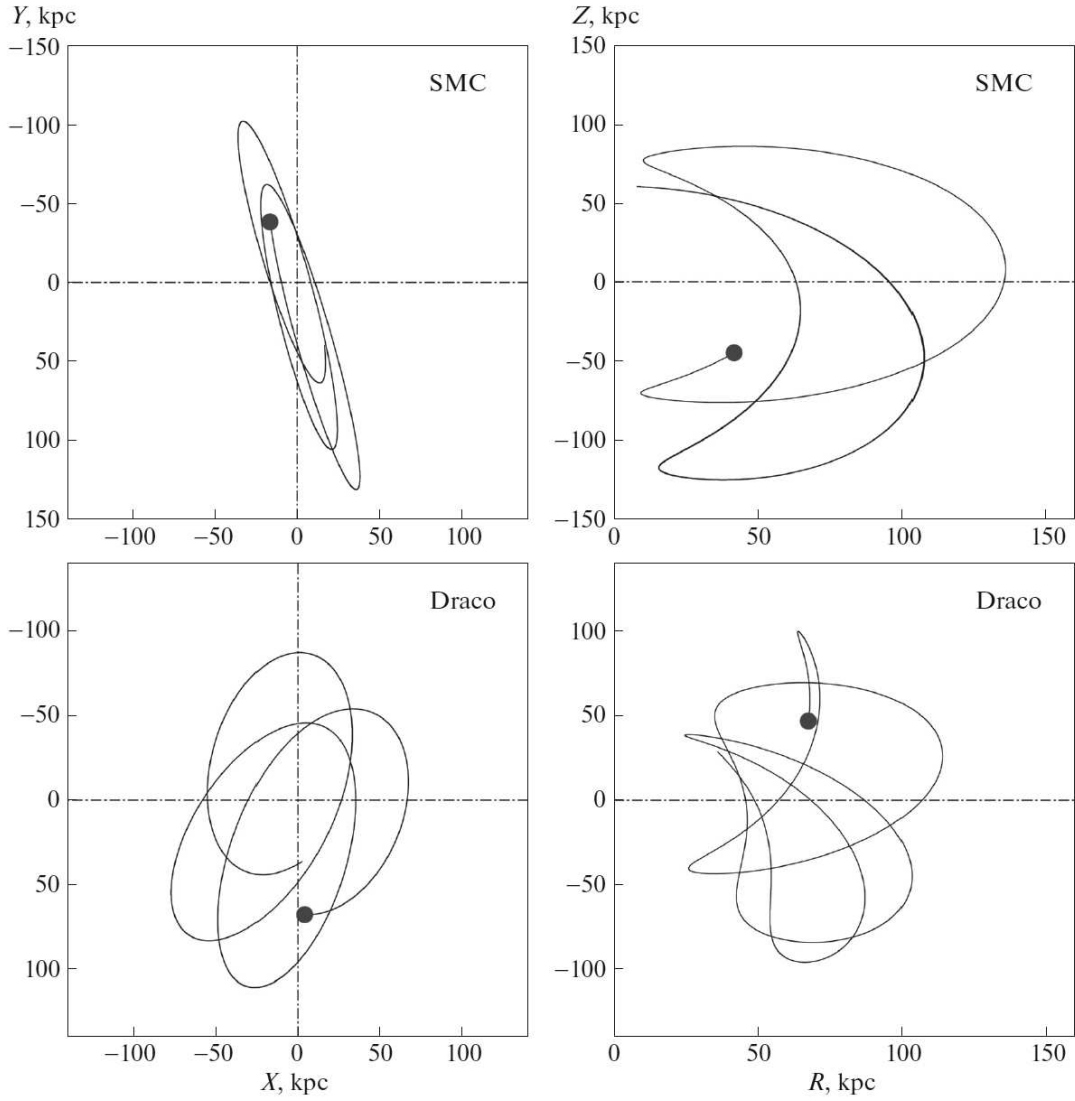


Figure 1: Galactic orbits of the dwarf galaxies SMC and Draco over 10 billion years into the past.

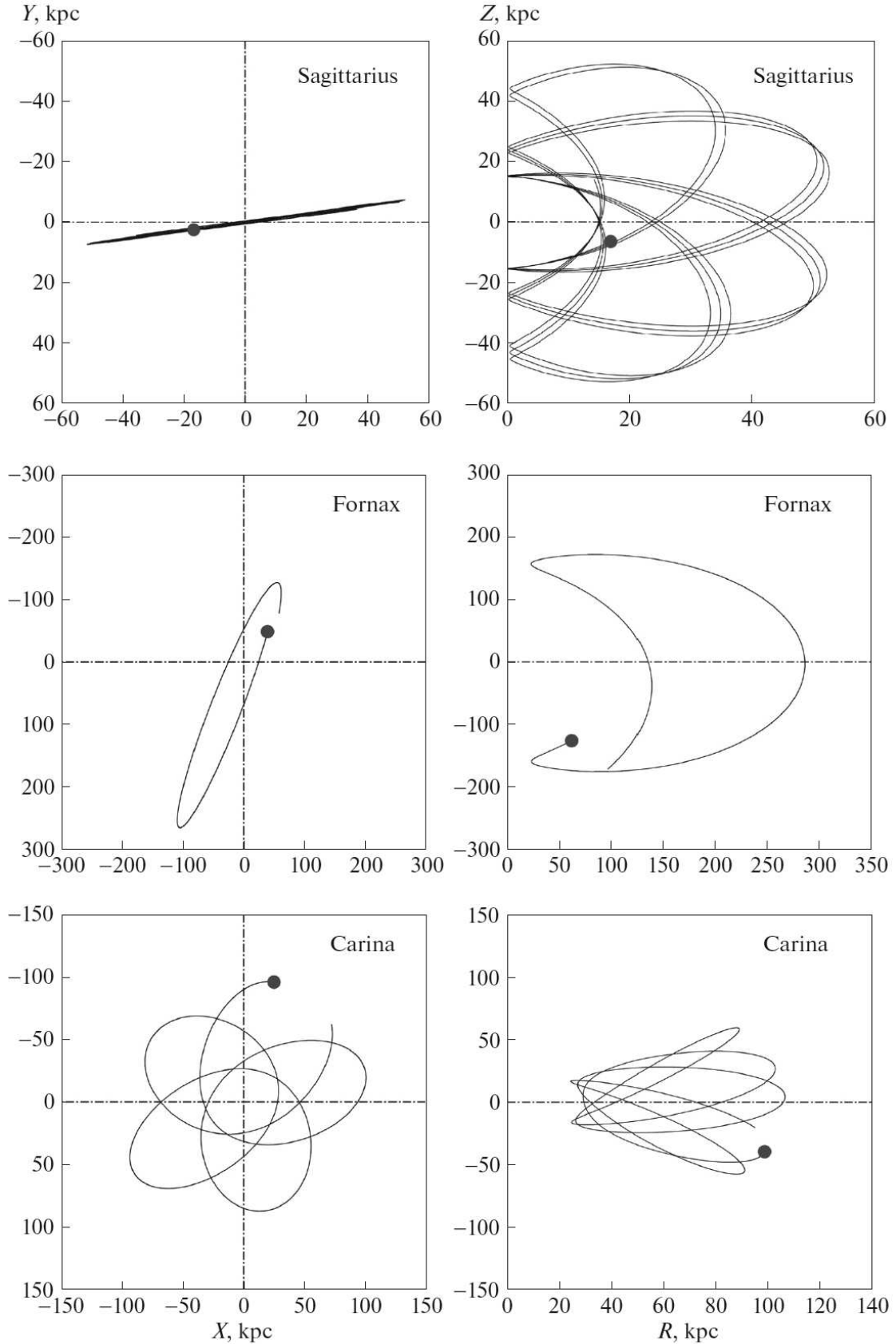


Figure 2: Galactic orbits of the dwarf galaxies Sagittarius, Fornax, and Carina over 10 billion years into the past.

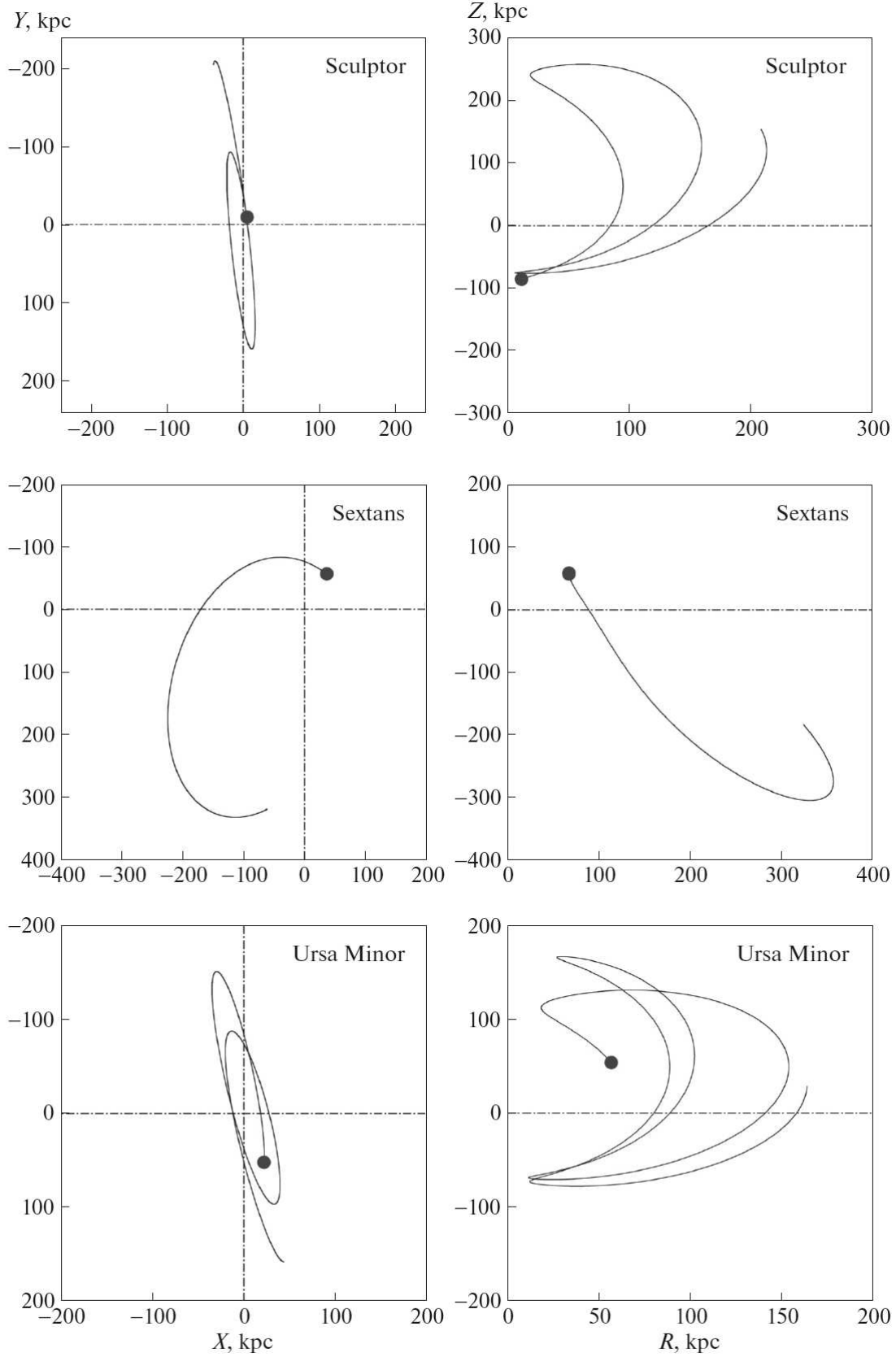


Figure 3: Galactic orbits of the dwarf galaxies Sculptor, Sextans, and Ursa Minor over 10 billion years into the past.

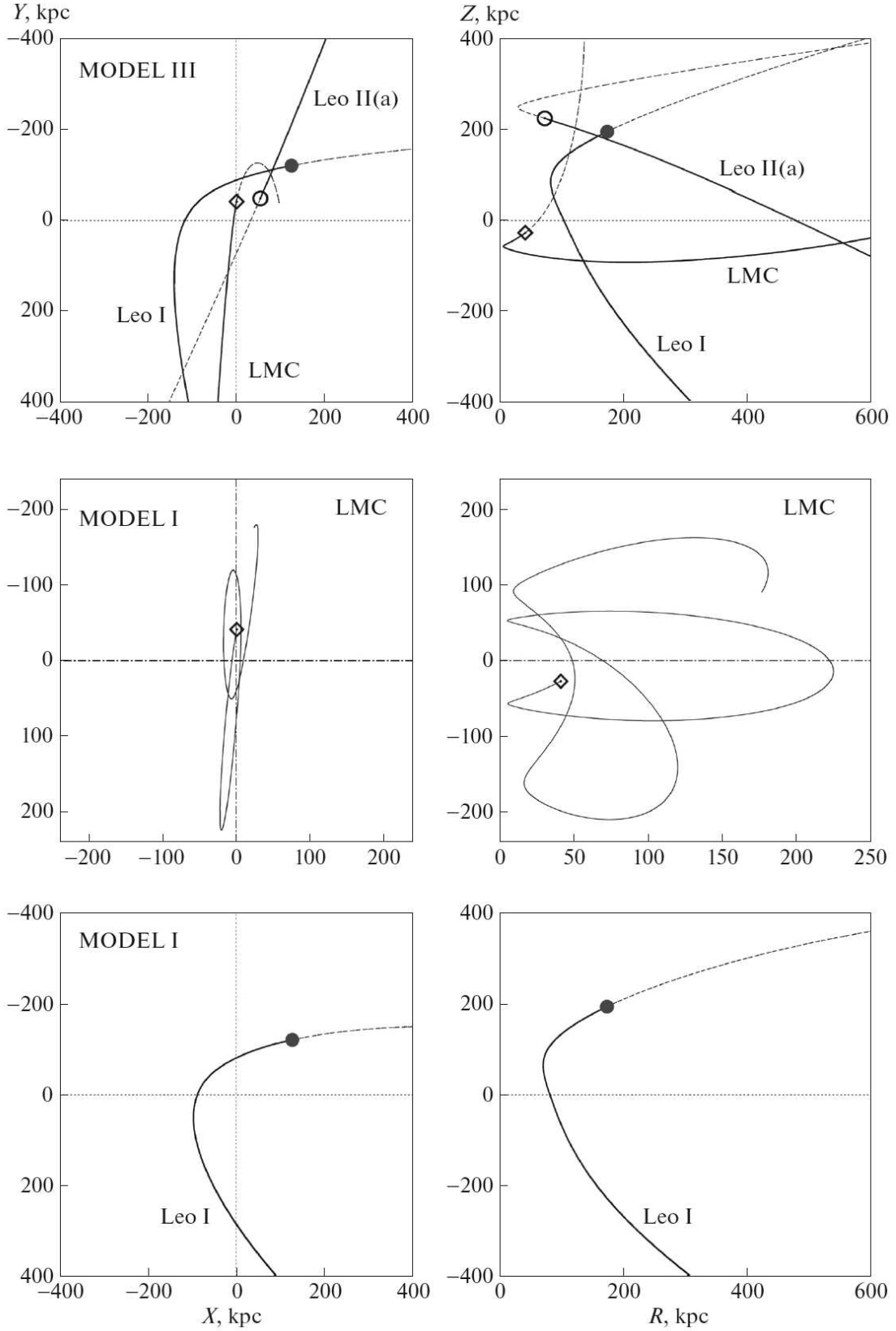


Figure 4: Galactic orbits of the dwarf galaxies LMC, Leo I, and Leo II (a) over 10 billion years into the past (solid curves) and 10 billion years into the future (dashed curves). The trajectories in the upper panel were computed using Model III for the Galactic potential; the two other panels show results for Model I (with a higher mass for the Galaxy).

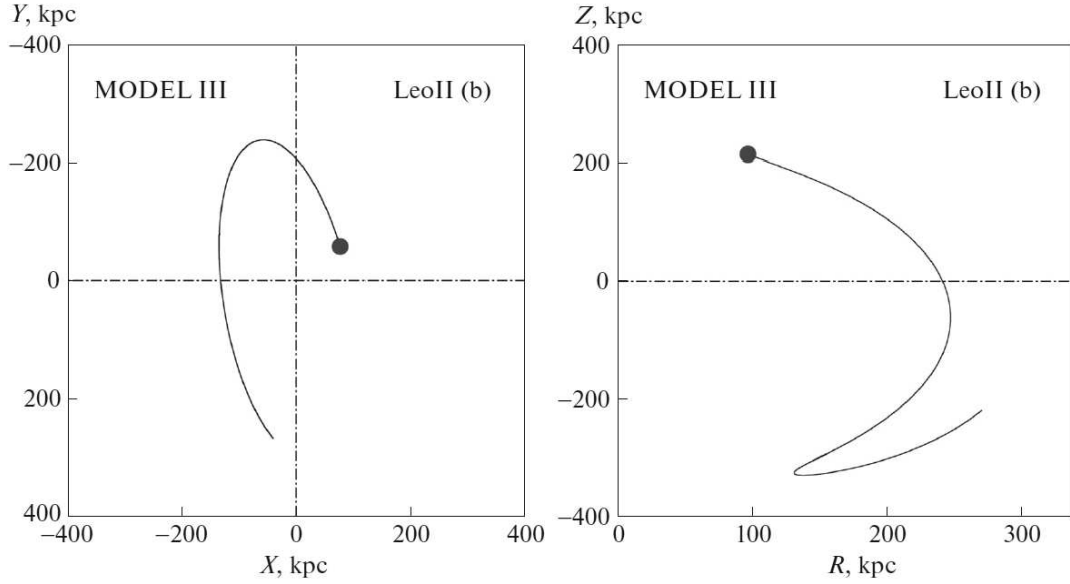


Figure 5: Galactic orbits of the dwarf galaxy Leo II (b) over 10 billion years into the past derived using Model III for the Galactic potential.

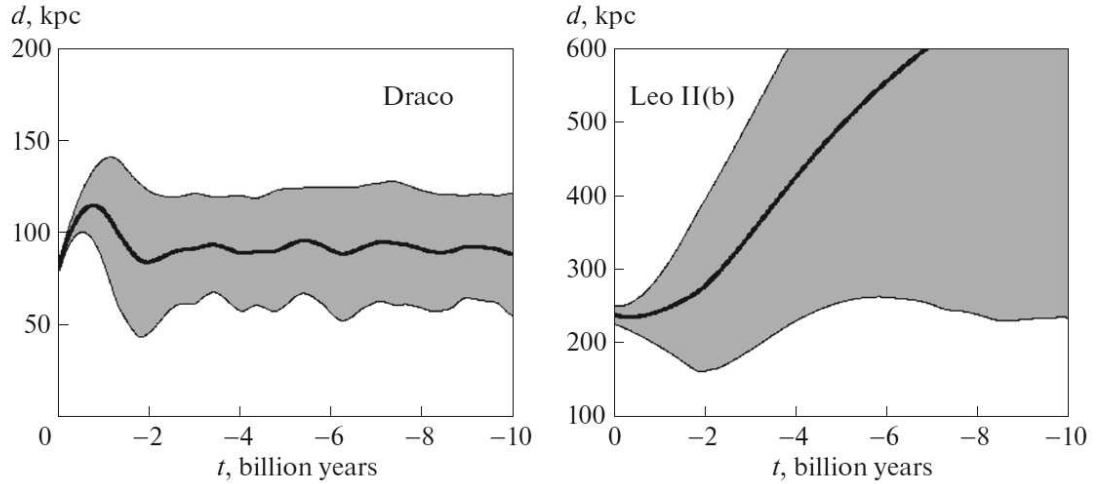


Figure 6: Distances to Draco and Leo II (solid curves) as a function of time, computed taking into account the uncertainties in the input data and gravitational-potential parameters; the shading shows the confidence area corresponding to the  $\pm 1\sigma$  uncertainties.

We see from the upper part of Table 4 that the motion of eight of the galaxies (Fornax, Sagittarius, Ursa Minor, Sculptor, Sextans, Draco, Carina, and SMC) demonstrates that they are gravitationally bound to the Milky Way. In particular, this is indicated by the comparatively low eccentricities of their orbits ( $e < 0.8$ ). This conclusion is based on an analysis of the galactic orbits computed using the gravitation potential with a comparatively low total mass,  $M_{200} = (0.75 \pm 0.19) \times 10^{12} M_{\odot}$ .

The upper part of Table 4 and Fig. 4 also show that the LMC, Leo I, and Leo II (a) have highly elongated orbits with eccentricities  $e > 0.8$ . In such cases, a potential with a higher mass for the Galaxy is usually applied (e.g., [4]), especially since estimates of the Galaxy's total mass lie in a fairly wide range:  $M_{200} = (0.4 - 2.0) \times 10^{12} M_{\odot}$  [17].

Some orbital characteristics of the Milky Way's companion galaxies were estimated in [5] using a model for the gravitation potential with a total mass of the Galaxy  $M_{200} = 1.1 \times 10^{12} M_{\odot}$ . As in our study, high eccentricities,  $e > 0.8$ , were obtained for the LMC, Leo I, and Leo II (a); see Fig. 8 in [5]. On the other hand, the orbit derived for Leo II (b) with the new proper motions has a low eccentricity,  $e = 0.23$ . The orbit of this galaxy derived using Model III is shown in Fig. 5.

The lower part of Table 4 presents the results obtained by applying Model I to the LMC and Leo I. Here, the total mass of the Galaxy is  $M_{200} = (1.45 \pm 0.30) \times 10^{12} M_{\odot}$ . This yielded a much less elongated orbit for the LMC. However, although the orbit of Leo I became smaller, it is still very elongated. Of course, it is possible to address this problem in the opposite sense, and determine the mass of the Galaxy for which Leo I would be gravitationally bound to the Milky Way. A fairly high mass for the Galaxy was obtained in [4] when considering a similar problem:  $M = 2.4 \times 10^{12} M_{\odot}$  for the sample with Leo I, or  $M = 1.7 \times 10^{12} M_{\odot}$  without Leo I.

Leo I has a very high radial velocity, indicating that it is only weakly bound to the Galaxy. It is interesting that the orbital characteristics for the LMC and Leo II (a) computed into the future are virtually the same as those for the orbits computed into the past. However, applying Model I to Leo I yields the orbital parameters  $a_{min} = 261$  kpc,  $a_{max} = 1082$  kpc, and  $e = 0.61$ . This leads us to expect that more accurate measurements for Leo I could significantly influence the character of its orbit, as occurred for Leo II.

The orbital parameters for all the dwarf-galaxy companions of the Milky Way we have analyzed, obtained taking into account the uncertainties in the input data and in the parameters of the Galaxy's gravitation potential, are presented in Table 5. As an example of two typical cases of how the uncertainties influence the orbits, Fig. 6 shows the distances to Draco and Leo II (b) and their confidence areas corresponding to the  $\pm 1\sigma$  level of uncertainties in the distances.

To determine the mean parameters and their rms deviations, we carried out statistical Monte Carlo simulations using 100 independent realizations of the random errors for each object, described by a normal law with zero mean and specified rms deviation. The results (Table 5) can be used to judge the extent to which a companion is gravitationally bound to the Galaxy, taking into account the measurement uncertainties. For example, the random errors have brought about a shift of the mean orbital eccentricity towards higher values relative to the nominal value for several of the galaxies (compare Tables 4 and 5); this is especially clear for Sextans. For most of the galaxies (Fornax, Sagittarius, Ursa Minor, Sculptor, Draco, Carina, the SMC), the character of their orbits testifies that they are tightly gravitationally bound to the Galaxy, even in the case of a comparatively small total mass for the Galaxy,  $M_{200} = 0.75 \times 10^{12} M_{\odot}$ , corresponding to the modified model for the gravitational

potential of Navarro, Frenk, and White [12].

### 3.4 CONCLUSIONS

We have compiled the results of high-accuracy measurements of proper motions, radial velocities, and distances for 11 galaxies in the Local Group from the literature. The most distant of these, Leo I, is 254 kpc from the Sun.

We have derived Galactic orbits for all 11 galaxies covering a long time interval. We mainly used the Navarro, Frenk, & White model for the Galactic potential, refined by us, with a comparatively small total mass for the Galaxy,  $M_{200} = 0.75 \times 10^{12} M_{\odot}$ . The character of the orbits of most of these galaxies (Fornax, Sagittarius, Ursa Minor, Sculptor, Draco, Carina, the SMC) demonstrates that they are tightly gravitationally bound to the Galaxy.

However, the orbits for some of the galaxies were found to be fairly elongated; for example, the orbital eccentricity derived for the LMC is  $e = 0.90$ . Using another model for the Galactic potential (the Allen-Santillán model, again refined by us), with a total mass for the Galaxy  $M_{200} = 1.45 \times 10^{12} M_{\odot}$ , we obtained a more compact orbit for the LMC with the eccentricity  $e = 0.65$ .

An exception is the galaxy Leo I, whose orbit is extremely elongated,  $e > 0.8$ , even using this latter model potential. Thus, the question of whether this galaxy is fully gravitationally bound to the Milky Way remains open.

### ACKNOWLEDGEMENTS

We thank the referee for useful comments that have helped to improve this paper. This work was supported by the Basic Research Program P-7 of the Presidium of the Russian Academy of sciences, under the subprogram “Transitional and Explosive Processes in Astrophysics”.

### REFERENCES

1. A.W. McConnachie, *Astron. J.* 144, 4 (2012).
2. J. D. Diaz, S. E. Koposov, M. Irwin, V. Belokurov, and N. W. Evans, *Mon. Not. R. Astron. Soc.* 443, 1688 (2014).
3. M. S. Pawlowski, S. S. McGaugh, and H. Jerjen, *Mon. Not. R. Astron. Soc.* 453, 1047 (2015).
4. M. I. Wilkinson and N. W. Evans, *Mon. Not. R. Astron. Soc.* 310, 645 (1999).
5. M. Rocha, A. H. G. Peter, and J. Bullock, *Mon. Not. R. Astron. Soc.* 425, 231 (2012).
6. H. Lux, J. I. Read, and G. Lake, *Mon. Not. R. Astron. Soc.* 406, 2312 (2010).
7. G. W. Angus, A. Diaferio, and P. Kroupa, *Mon. Not. R. Astron. Soc.* 416, 1401 (2011).
8. C. Barber, E. Starkeburg, J. F. Navarro, A. W. McConnachie, and A. Fattahi, *Mon. Not. R. Astron. Soc.* 437, 959 (2014).
9. S. Lépine, A. Koch, R. M. Rich, and K. Kuijken, *Astrophys. J.* 741, 100 (2011).
10. M. S. Pawlowski and P. Kroupa, *Mon. Not. R. Astron. Soc.* 435, 2116 (2013).
11. R. P. van der Marel, *Galaxy Masses as Constraints of Formation Models*, Ed. by M. Cappellari and S. Courteau (Cambridge University Press, 2015), p. 1.
12. A. T. Bajkova and V. V. Bobylev, *Astron. Lett.* 42, 567 (2016).
13. C. Allen and A. Santillán, *Rev. Mex. Astron. Astrofis.* 22, 255 (1991).
14. M. I. Wilkinson and N. W. Evans, *Mon. Not. R. Astron. Soc.* 310, 645 (1999).
15. J. F. Navarro, C. S. Frenk, and S. D. M. White, *Astrophys. J.* 490, 493 (1997).

16. M. Miyamoto and R. Nagai, *Publ. Astron. Soc. Jpn.* 27, 533 (1975).
17. P. Bhattacharjee, S. Chaudhury, and S. Kundu, *Astrophys. J.* 785, 63 (2014).
18. C. Pryor, S. Piatek, and E. W. Olszewski, *Astron. J.* 149, 42 (2015).
19. D. I. Casetti-Dinescu and T. M. Girard, *Mon. Not. R. Astron. Soc.* 461, 271 (2016).
20. K. Kinemuchi, H. C. Harris, H. A. Smith, N. A. Silbermann, L. A. Snyder, A. P. LaCluyzé, and C. L. Clark, *Astron. J.* 136, 1921 (2008).
21. T. E. Armandroff, E. W. Olszewski, and C. Pryor, *Astron. J.* 110, 2131 (1995).
22. R. P. van der Marel and J. Sahlmann, *Astrophys. J.* 832, L23 (2016).
23. R. P. van der Marel and N. Kallivayalil, *Astrophys. J.* 781, 121 (2014).
24. A. G. A. Brown, A. Vallenari, T. Prusti, J. H. J. de Bruijne, et al., *Astron. Astrophys.* 595, 2 (2016).
25. L. Lindgren, U. Lammers, U. Bastian, J. Hernandez, et al., *Astron. Astrophys.* 595, 4 (2016).
26. S. Piatek, C. Pryor, and E. W. Olszewski, *Astron. J.* 152, 166 (2016).
27. A. Koch, J. T. Kleyna, M. I. Wilkinson, E. K. Grebel, G. F. Gilmore, N. Wyn Evans, R. F. G. Wyse, and D. R. Harbeck, *Astron. J.* 34, 566 (2007).
28. M. Bellazzini, N. Gennari, and F. R. Ferraro, *Mon. Not. R. Astron. Soc.* 360, 185 (2005).
29. A. Irrgang, B. Wilcox, E. Tucker, and L. Schiefelbein, *Astron. Astrophys.* 549, 137 (2013).
30. R. Schönrich, J. Binney, and W. Dehnen, *Mon. Not. R. Astron. Soc.* 403, 1829 (2010).